UNIVERSITY OF MINNESOTA
ST. ANTHONY FALLS LABORATORY
Engineering, Environmental and Geophysical Fluid Dynamics

Project Report No. 443

Certain Computational Aspects of Modeling Stratified Environmental/Geophysical Flows Pertaining to Lakes

by

Dragoslav L. Stefanovic and Heinz G. Stefan

Prepared for

MINNESOTA DEPARTMENT OF NATURAL RESOURCES
Metro Region Fisheries, St. Paul, Minnesota

March 2000
Minneapolis, Minnesota

Prepared for: MN Dept. of Natural Resources
Last Revised: 3/17/00
Disk Locators: PR443cov.doc; PR443.doc;
(Zip Disk #15\Drag)/Stefan Reports

TABLE OF CONTENTS

ABSTRACT

Two intricate issues related to environmental hydrodynamics and water quality numerical modeling, with specific application to lakes, are addressed in this report: turbulent closure for stratified flows and transformation of the physical domain into a computational domain. Both problems are very important for the development of an accurate and efficient numerical algorithm intended to simulate thermo-hydrodynamics and transport processes in a lake (pond) cross section. The first section of the report considers the state-of-the art in turbulence modeling of environmental/geophysical flows (e.g. lakes, oceans, atmosphere) particularly in stratified ambiences, where the vertical turbulent transport is significantly hindered by density stratification. The findings and recommendations stemming from this investigation are reported herein. In the second section of the report, the numerical treatment of irregular lake geometry is described in detail and a simple, efficient mapping transformation is proposed to facilitate the computation in a lake cross section of an arbitrary form.

ACKNOWLEDGMENT

The work reported herein was supported by the Minnesota Department of Natural Resources, Metro Region Fisheries, as part of a project study on dissolved oxygen dynamics in Holland Lake, MN. Mr. Gerald Johnson was the project officer. The methodology developed and described in this report is intended for use in lake thermo-hydrodynamics and water quality modeling. We are grateful for having an opportunity to develop and validate new modeling concepts related to an important ecological issue such as dissolved oxygen dynamics in lakes.

LIST OF FIGURES

I. TURBULENCE CLOSURE FOR STRATIFIED ENVIRONMENTAL/GEOPHYSICAL FLOWS WITH APPLICATION TO LAKES

I.1. INTRODUCTION

In most geophysical flows (e.g. lakes, oceans, atmosphere), the largest scales of fluid motion are determined by the geometry of the flow regime and the smallest by the viscosity of the fluid. It is practically impossible to simulate the development in space and time of this full range of scales because of the huge computational resources required. The only practical solution to this problem is to describe the flow in terms of some sort of average of the flow variables. Using ensemble and time averages has been the traditional way of studying and describing turbulent flows. The term "conventional" will be used to refer to this approach. Another alternative is to work with space averages of the field variables and simulate their time history. Motion of scales smaller than the size of the space-averaging operator are then characterized as subgrid scale (SGS) turbulence. This approach in description of turbulent flows is usually referred to as the Large Eddy Simulation (LES) method. The use of both conventional and LES methods in lake hydrodynamics simulation was considered. The findings and recommendations stemming from that investigation are rationalized below.

I-2. CONVENTIONAL TURBULENCE MODELING

Conventional turbulence treatment resorts to statistical averaging of flow properties, so that the governing equations of motion (the Navier-Stokes equations) are solved only for the mean-flow quantities. However, the process of averaging creates a new problem: the equations no longer constitute a closed system as they contain unknown terms representing the transport of mean momentum, heat and mass by the turbulent motion. The system can be closed only with the aid of empirical input, hence the calculation methods based on the averaged flow equations are semi-empirical. A turbulence model is then defined as a set of equations (algebraic or differential) which determine the turbulent transport terms in the mean-flow equations and thus close the system of equations. Many of the models of this kind are based on the eddy-viscosity/eddy-diffusivity concept for modeling the turbulent or Reynolds stresses. The use of this concept for closing the system of statistically averaged equations of motion, which are (originally) developed for laminar flow, is outlined below.

For a two dimensional flow, the time averaged equations of conservation of linear momentum, mass and thermal energy in the vorticity-stream function formulation can be written as follows

$$\frac{\partial \overline{\omega}}{\partial t}+\frac{\partial \overline{u}\overline{\omega}}{\partial x}+\frac{\partial \overline{v}\overline{\omega}}{\partial y}=\nu\left(\frac{\partial^2 \overline{\omega}}{\partial x^2}+\frac{\partial^2 \overline{\omega}}{\partial y^2}\right)-g\beta\frac{\partial \overline{T}}{\partial x}-\left(\frac{\partial^2}{\partial x^2}-\frac{\partial^2}{\partial y^2}\right)\overline{u'v'}-\frac{\partial^2}{\partial x\partial y}\left(\overline{v'^2}-\overline{u'^2}\right) \tag{1}$$

$$\frac{\partial^2 \overline{\psi}}{\partial x^2}+\frac{\partial^2 \overline{\psi}}{\partial y^2}=-\overline{\omega} \tag{2}$$

$$\frac{\partial \overline{T}}{\partial t}+\frac{\partial \overline{u}\overline{T}}{\partial x}+\frac{\partial \overline{v}\overline{T}}{\partial y}=\alpha\left(\frac{\partial^2 \overline{T}}{\partial x^2}+\frac{\partial^2 \overline{T}}{\partial y^2}\right)-\frac{\partial}{\partial x}\left(\overline{u'T'}\right)-\frac{\partial}{\partial y}\left(\overline{v'T'}\right) \tag{3}$$

with $\overline{u}=\partial\overline{\psi}/\partial y$ and $\overline{v}=-\partial\overline{\psi}/\partial x$. The mean quantities are defined as $\overline{\phi}=\frac{1}{\Delta t}\int_t^{t+\Delta t}\phi dt$ where the averaging time Δt is long compared to the time scale of the turbulent motion and small compared to the time scale of the mean flow. Boussinesq's eddy-viscosity concept assumes that, in analogy to the viscous stresses in laminar flows, the turbulent (Reynolds) stresses are proportional to the mean-velocity gradients. For general flow situations, this concept may be expressed in tensor notation as (Rodi 1980)

$$-\overline{u_i' u_j'}=\nu_t\left(\frac{\partial \overline{u}_i}{\partial x_j}+\frac{\partial \overline{u}_j}{\partial x_i}\right)-\frac{2}{3}k\delta_{ij} \tag{4}$$

where $k=0.5\,\overline{u_i' u_i'}$ is the kinetic energy of the fluctuating motion, δ_{ij} is the Kronecker delta and ν_t is the turbulent eddy viscosity which, in contrast to the molecular viscosity ν, is not a fluid property but depends strongly on the state of turbulence. The introduction of Eq. (4) alone does not constitute a turbulence model but only provides the framework for constructing such a model. Apparently, the main problem is now shifted to determining the distribution of ν_t. The eddy-viscosity defined by Eq. (4) was conceived by presuming an analogy between the molecular motion, which leads to Stokes' viscosity law in laminar flow, and the turbulent motion. In spite of this conceptual inadequacy, the eddy-viscosity formulation has proved successful in many practical calculations and is still the basis of most turbulence models in use today.

In direct analogy to the turbulent momentum transport, the turbulent heat/mass transport is often assumed to be related to the gradient of the transported quantity ϕ

$$-\overline{u_i' \phi'}=\Gamma\frac{\partial \overline{\phi}}{\partial x_i} \tag{5}$$

where Γ is the turbulent diffusivity of heat or mass. Like the eddy viscosity, Γ is not a fluid property but depends on the state of the turbulent motion. The Reynolds analogy between heat/mass transport and momentum transport suggests that Γ is closely related to ν_t. Their ratio $\sigma_t=\nu_t/\Gamma$ is called the turbulent Prandtl number (for heat) or Schmidt number (for mass) number and, unlike their laminar counterpart, varies only little across a flow and from flow to flow (Rodi 1980). Therefore, many models make use of Eq. (5) with the turbulent Prandtl/Schmidt number as a constant, not much different from one.

The simplest models for determining the distribution of ν_t over the flow field relate the eddy viscosity directly to the mean-velocity distribution (e.g. the local gradient). These models implicitly assume that the turbulence is dissipated where it is generated, which means that there is no transport of turbulence in the flow field. In cases where the state of turbulence at a point is influenced significantly by the turbulence generation somewhere else in the flow (e.g. recirculating cavity flows), the simple models neglecting turbulence transport are inadequate. In order to account for the transport of turbulence, models have been developed which employ transport equations for quantities characterizing the turbulence. As the eddy viscosity is proportional to a velocity scale $\hat{V}$ and a length scale $\hat{L}$ characterizing the (large scale) turbulent motion, advanced turbulence models usually use a transport equation for the single velocity scale with or without a transport equation for the single length scale. Thus, it has become customary to classify turbulence models according to the number of transport equations used for turbulence quantities.

Regardless of the kind of the turbulence closure used, it is necessary to account for turbulence anisotropy in stratified flows. It is well known that the vertical turbulent transport of both momentum and scalar quantities is strongly influenced by buoyancy forces. In particular, the eddy viscosity and diffusivity can be significantly reduced by stable stratification. In the simple models used (constant eddy viscosity/diffusivity), this buoyancy influence is accounted for by a Richardson number via empirical formulae (Rodi 1980)

$$\begin{aligned} \nu_{tz} &= \nu_{tz}^{o}(1+\beta R_i)^{\alpha} \\ \Gamma_z &= \Gamma_z^{o}(1+\beta_\phi R_i)^{\alpha_\phi} \end{aligned} \qquad (6)$$

where $R_i = -\dfrac{g\partial\rho/\partial z}{\rho(\partial u/\partial z)^2}$ is the gradient Richardson number, which is the ratio of gravity to inertial forces and characterizes the importance of buoyancy effects, ν_{tz}^{o} and Γ_z^{o} are respectively the values of ν_{tz} and Γ_z for neutral stratification (R_i = 0). The Munk-Anderson (1948) coefficients $\alpha = -0.5$, $\beta = 10$, $\alpha_\phi = -1.5$ and $\beta_\phi = 3.33$ have been found to fit environmental experimental data. Other formulations in place of equation (6) have also been proposed (Turner 1973, Liggett 1976).

I.2.1. Two-Equation (k-ε) Model

If the velocity fluctuations are to be characterized by one scale, the physically most meaningful scale is $\sqrt{k}$, where $k = 0.5\,\overline{u_i' u_i'}$ is the kinetic energy of the turbulent motion (per unit mass). As the energy k is contained mainly in the large-scale fluctuations, $\sqrt{k}$ is a velocity scale for the large scale turbulent motion. When this scale is used to define the eddy viscosity, the Kolmogorov-Prandtl expression results

$$\nu_t = c_\mu' \sqrt{k}\hat{L} \qquad (7)$$

where c_μ' is an empirical constant and $\hat{L}$ is a characteristic length scale. The distribution of k can be determined by solving a transport equation for this quantity. Such an equation can be derived from the Navier-Stokes equation in the exact form, as follows

$$\frac{\partial k}{\partial t}+\underbrace{\overline{u}_i\frac{\partial k}{\partial x_i}}_{C}=\underbrace{\frac{\partial}{\partial x_i}\left[\overline{u_i'\left(\frac{u_j'u_j'}{2}+\frac{p}{\rho}\right)}\right]}_{D}-\underbrace{\overline{u_i'u_j'}\frac{\partial \overline{u}_i}{\partial x_j}}_{P}-\underbrace{\beta g_i\overline{u_i'T'}}_{G}-\underbrace{\nu\overline{\frac{\partial u_i'}{\partial x_j}\frac{\partial u_i'}{\partial x_j}}}_{\varepsilon} \tag{8}$$

Equation (8) states that the rate of change of k is balanced by the convective transport due to the mean motion (C), the diffusive transport due to velocity and pressure fluctuations (D), the production (P) of k by interaction of Reynolds stresses and mean-velocity gradients, the production/destruction (G) of k due to buoyancy effects and the dissipation (ε) of k by viscous action into heat. The production term P represents the transfer of kinetic energy from the mean to the turbulent motion. The buoyancy term G represents an exchange between the turbulent kinetic energy k and potential energy. In stable stratification this term becomes positive so that k is reduced and the turbulence is damped while the potential energy of the system increases. In unstable stratification turbulent energy is produced at the expense of potential energy. The viscous dissipation ε transfers kinetic energy into internal energy of the fluid and is always a sink term.

The exact k-equation (8) is of no use in a turbulence model unless some model assumptions are introduced for new unknown correlations in the diffusion and dissipation terms. It is customary to assume that the diffusion flux of k is proportional to the gradient of k in the following manner

$$\overline{u_i'\left(\frac{u_j'u_j'}{2}+\frac{p}{\rho}\right)}=\frac{\nu_t}{\sigma_k}\frac{\partial k}{\partial x_i} \tag{9}$$

where σ_k is an empirical diffusion constant. The dissipation ε is usually modeled by the expression

$$\varepsilon=c_D\frac{k^{3/2}}{\hat{L}} \tag{10}$$

where c_D is a further empirical constant. It is seen that the rate of dissipation is governed by the large-scale motion characterized by the parameter $\hat{L}$, even though the dissipation takes place at the smallest eddies.

With the above model assumptions and the eddy viscosity/diffusivity expressions for $\overline{u_i'u_j'}$ and $\overline{u_i'T'}$, the k-equation reads

$$\frac{\partial k}{\partial t}+\overline{u}_i\frac{\partial k}{\partial x_i}=\frac{\partial}{\partial x_i}\left(\frac{\nu_t}{\sigma_k}\frac{\partial k}{\partial x_i}\right)+\underbrace{\nu_t\left(\frac{\partial \overline{u}_i}{\partial x_j}+\frac{\partial \overline{u}_j}{\partial x_i}\right)\frac{\partial \overline{u}_i}{\partial x_j}}_{P}+\underbrace{\beta g_i\frac{\nu_t}{\sigma_t}\frac{\partial \overline{T}}{\partial x_i}}_{G}-\underbrace{c_D\frac{k^{3/2}}{\hat{L}}}_{\varepsilon} \tag{11}$$

To complete the turbulence model it is necessary to specify the length scale $\hat{L}$. In many models $\hat{L}$ is determined from simple empirical relations similar to those given for the Prandtl mixing length. These prescriptions work well in certain simple flows and flow geometries (e.g. wall-boundary layers, channel flows, free jets), but for more complex (recirculating) flows they are of little use. Therefore, the trend has been to move on to two-equation models which determine the length scale from a transport equation. The rationale behind this is the fact that the

length scale of the large (energy-containing) eddies is subject to transport processes similar to those for the energy k. For example, the eddies generated at one place are convected downstream so that their size at any station depends on their initial size. Other processes involved are dissipation, which destroys the small eddies and thus effectively increases the mean eddy size and vortex stretching connected with the energy cascade, which reduces the mean eddy size. A length-scale equation need not necessarily have the length scale itself as dependent variable; any combination of the form $Z = k^m \hat{L}^n$ would suffice, because k is known from solving the k-equation (11). In fact, most equations proposed do not use $\hat{L}$, and one of the most popular transport equations is the one for the dissipation rate $\varepsilon \sim k^{3/2}/\hat{L}$. This equation can be derived in the exact form from the Navier-Stokes equations for the fluctuating vorticity at high Reynolds numbers (local isotropy). In order to make the equation tractable, some drastic model assumptions are required for the complex correlations whose behavior is still little known. The outcome of the modeling of the diffusion, generation and destruction terms in the exact equation is the ε-equation presented below (Rodi 1980)

$$\frac{\partial \varepsilon}{\partial t} + \bar{u}_i \frac{\partial \varepsilon}{\partial x_i} = \frac{\partial}{\partial x_i}\left(\frac{\nu_t}{\sigma_\varepsilon}\frac{\partial \varepsilon}{\partial x_i}\right) + c_1 \frac{\varepsilon}{k}(P+G) - c_2 \frac{\varepsilon^2}{k} \tag{12}$$

where σ_ε is another empirical constant and P and G are the production and buoyancy terms from the k-equation (11). The equations for eddy viscosity/diffusivity, derived from Eqs. (7) and (10) and from the definition of the turbulent Prandtl number, finally complete the two-equation turbulence model

$$\nu_t = c_\mu \frac{k^2}{\varepsilon}, \quad \Gamma = \frac{\nu_t}{\sigma_t} \tag{13}$$

The following "universal" constants have been derived from experimental data and proposed by Launder and Spalding (1974)

$$c_\mu = 0.09, \; c_1 = 1.44, \; c_2 = 1.92, \; \sigma_k = 1.0, \; \sigma_\varepsilon = 1.3$$

The k-ε model, in the form described above, has been applied successfully to many two-dimensional wall boundary layers, duct flows, free shear and recirculating flows. However, some modification of constants is suggested for nonisotropic situations, especially pertaining to buoyancy-induced flows. One such modification is proposed by Rodi (1980) for the coefficient c_1 in the form

$$c_1 = 1.44\,(1 + c_3 R_f), \quad R_f = -\frac{G}{P}, \; c_3 \approx 0.8 \tag{14}$$

Another possibility is to use the algebraic-stress-model approach by deriving transport equations for the stresses $\overline{u_i' u_j'}$ and $\overline{u_i' T'}$, which are then simplified to yield algebraic relations. The transport equations contain buoyancy terms which appear also in the algebraic relations, leading effectively to non-isotropic eddy viscosities and diffusivities as functions of some local Richardson number. This approach will be discussed later in this review under the Mellor-Yamada turbulence closure model.

The use of the aforementioned k-ε turbulence model for closing the Reynolds equations of motion in the vorticity-stream function form (Eqs. 1-3), is illustrated on the case of natural convection in a differentially heated rectangular cavity (Fig. I-1). This problem is a standard test case for more complex recirculating flows in a natural lake cross section. Using the following non-dimensional variables

$$\xi=\frac{x}{L}\ ,\ \eta=\frac{y}{H},\quad \tau=\frac{\nu}{HL}t,\quad T=2\frac{\overline{T}-T_M}{T_H-T_C},\quad u=\frac{H}{\nu}\overline{u},\quad v=\frac{L}{\nu}\overline{v},\quad \psi=\frac{\overline{\psi}}{\nu},\quad \omega=\frac{LH}{\nu}\overline{\omega},$$

$$k=\frac{HL}{\nu^2}\mathrm{k},\quad \varepsilon=\frac{H^2L^2}{\nu^3}\varepsilon,\quad \gamma=\frac{\nu_t}{\nu},\quad T_M=\frac{1}{2}(T_C+T_H)$$

and with the Reynolds stresses and turbulent heat fluxes evaluated respectively by equations (4) and (5), the following closed system of equations describes a turbulent, buoyancy-driven two-dimensional flow

$$\frac{\partial\omega}{\partial\tau}+\frac{\partial u\omega}{\partial\xi}+\frac{\partial v\omega}{\partial\eta}=c\frac{\partial^2\omega}{\partial\xi^2}+\frac{1}{c}\frac{\partial^2\omega}{\partial\eta^2}-c^2\frac{Gr}{2}\frac{\partial T}{\partial\xi}+\frac{\partial^2}{\partial\xi^2}\left[\gamma\left(\frac{\partial u}{\partial\eta}+c^2\frac{\partial v}{\partial\xi}\right)\right]$$
$$-\frac{\partial^2}{\partial\eta^2}\left[\gamma\left(\frac{\partial v}{\partial\xi}+\frac{1}{c^2}\frac{\partial u}{\partial\eta}\right)\right]-\frac{\partial^2}{\partial\xi\partial\eta}\left[2\gamma\left(\frac{\partial u}{\partial\xi}-\frac{\partial v}{\partial\eta}\right)\right] \tag{15}$$

$$c\frac{\partial^2\psi}{\partial\xi^2}+\frac{1}{c}\frac{\partial^2\psi}{\partial\eta^2}=-\omega \tag{16}$$

$$\frac{\partial T}{\partial\tau}+\frac{\partial uT}{\partial\xi}+\frac{\partial vT}{\partial\eta}=c\frac{\partial}{\partial\xi}\left[\left(\frac{1}{Pr}+\frac{\gamma}{\sigma_t}\right)\frac{\partial T}{\partial\xi}\right]+\frac{1}{c}\frac{\partial}{\partial\eta}\left[\left(\frac{1}{Pr}+\frac{\gamma}{\sigma_t}\right)\frac{\partial T}{\partial\eta}\right] \tag{17}$$

$$\frac{\partial k}{\partial\tau}+\frac{\partial uk}{\partial\xi}+\frac{\partial vk}{\partial\eta}=c\frac{\partial}{\partial\xi}\left[\left(1+\frac{\gamma}{\sigma_k}\right)\frac{\partial k}{\partial\xi}\right]+\frac{1}{c}\frac{\partial}{\partial\eta}\left[\left(1+\frac{\gamma}{\sigma_k}\right)\frac{\partial k}{\partial\eta}\right]+\underbrace{c\frac{\gamma}{\sigma_t}\frac{Gr}{2}\frac{\partial T}{\partial\eta}}_{G}$$
$$+\underbrace{\gamma\left[2\left(\frac{\partial u}{\partial\xi}\right)^2+\left(\frac{1}{c}\frac{\partial u}{\partial\eta}+c\frac{\partial v}{\partial\xi}\right)^2+2\left(\frac{\partial v}{\partial\eta}\right)^2\right]}_{P}-\varepsilon \tag{18}$$

$$\frac{\partial\varepsilon}{\partial\tau}+\frac{\partial u\varepsilon}{\partial\xi}+\frac{\partial v\varepsilon}{\partial\eta}=c\frac{\partial}{\partial\xi}\left[\left(1+\frac{\gamma}{\sigma_\varepsilon}\right)\frac{\partial\varepsilon}{\partial\xi}\right]+\frac{1}{c}\frac{\partial}{\partial\eta}\left[\left(1+\frac{\gamma}{\sigma_\varepsilon}\right)\frac{\partial\varepsilon}{\partial\eta}\right]+\frac{\varepsilon}{k}(c_1P+c_3G)-c_2\frac{\varepsilon^2}{k} \tag{19}$$

$$\gamma=c_\mu\frac{k^2}{\varepsilon} \tag{20}$$

where $u=\partial\psi/\partial\eta$, $v=-\partial\psi/\partial\xi$, Prandtl number $Pr=\nu/\alpha$ and Grashof number $Gr=g\beta(T_H-T_C)L^3/\nu^3$.

The previous set of equations is solved by a numerical algorithm described for laminar flow (Stefanovic and Stefan 1999), where the wall-boundary conditions for the flow variables are also specified. Here, the vertical cavity walls are differentially heated (Fig. I-1), with constant temperature T_H along the warm wall ($x = 0$) and T_M along the cold wall ($x = L$). The horizontal walls ($y = 0$, $y = H$) are either insulated or have linear distribution of temperature. Boundary conditions $k = 0$ are normally specified at the walls, while the boundary conditions for ε are not imposed on the walls. Instead, using the Prandtl mixing length hypothesis, it can be estimated (Fraikin et al. 1980) for the first grid points from the wall

$$\varepsilon_1 = \frac{c_\mu^{3/4}}{\kappa} \frac{k_1^{3/2}}{\Delta_1} \tag{21}$$

where Δ_1 is the dimension of the first mesh of the grid and von Karman's constant $\kappa = 0.41$.

The irregular (hyperbolic) grid, used previously for the laminar flow simulation (Papanicolaou and Jaluria 1995), with denser distribution of grid points near the walls where the large gradients occur, is employed. The numerical results are obtained for a range of Grashof numbers Gr = 10^6, 10^8, 10^{10} and 10^{12}. The computational procedure covers the whole range of time-dependent solutions, beginning from the isothermal initial condition T= T_M. A typical transient result for the highest Grashof number (Gr = 10^{12}) is shown in Fig. I-2 in terms of the mean stream function contours and velocity vectors. The high complexity of the buoyancy-induced flow field, with a number of vortices of different strength, is apparent. These strongly recirculating flows are characterized by the momentum and viscous effects being of the same order, which requires special attention in preventing the likely emergence of numerical diffusion or dispersion. In addition, buoyancy force reversals, bi-directional velocity distributions and total convective inversions are commonly encountered, all of which renders this kind of flow difficult for accurate numerical simulation. Steady-state results for the dimensionless temperature (T), velocity vectors (V) and eddy viscosity (γ) are shown in Figures I-3 through I-5. A stable horizontal stratification exists in the middle of the cavity for Gr > 10^6 (Fig. I-3) and is more pronounced as the Grashof number increases. The horizontal temperature gradients are high in the vertical boundary layers while the vertical ones are high in the middle of the cavity. The velocities in the middle of the cavity (Fig. I-4) are very low compared to the velocities in the boundary layers. The horizontal boundary layers are thicker than the vertical ones. There is a strong recirculation along the left vertical (hot) wall, which is closer to the wall as the Grashof number increases. The distribution of the eddy viscosity is shown in Fig. I-5. For Gr = 10^6 the eddy viscosity is negligible compared to the molecular viscosity and the flow is essentially laminar. As the Grashof number increases, the turbulence level rises, especially in the lower left (upper right) corner of the cavity. Its value is 5, 25 and 100 times the molecular viscosity for Gr = 10^8, 10^{10} and 10^{12}, respectively. There is a second maximum on the top of the left vertical layer (at the bottom of the right vertical layer). It is evident that the eddy viscosity becomes significant near the outer edges of the boundary layers, while in the middle of the cavity the flow is essentially laminar. This result is a direct consequence of stable density stratification established in the middle of the cavity, where the buoyancy term G from the k-equation (Eq. 18) is negative, causing significant dissipation rather than production of turbulent kinetic energy. On the other hand, near the lower left (upper right) corner G is positive, contributing to shear production P of turbulent kinetic energy. The second maximum of the eddy viscosity in the vertical boundary layer is explained by the relative importance of shear production P due to the presence of

maximum velocity in that portion of the flow. All these findings are in good agreement with the numerical results of Fraikin et al. (1980). They are also compliant with the experiments performed by the same authors, corroborating the appearance of a turbulent area in the lower left/upper right corner of the cavity, while the rest of the flow was found to be laminar.

This study demonstrates that the application of the buoyancy extended k-ε model to an enclosed stratified flows is capable of providing physically plausible results, especially in the fully turbulent situations ($Gr > 10^8$) when there are two important sources of turbulent kinetic energy, namely buoyancy and shear. However, numerical simulations for high Grashof numbers revealed that the k-ε model is not easily manageable from the computational point of view. It was found that the addition of two highly nonlinear, coupled transport equations for k and ε (Eqs. 18 and 19) imposes severe limitation on the computational time step, making it almost two orders of magnitude smaller than the allowable time step for the laminar case. The model also requires a large number of grid points to assure convergence of the results. Special attention is necessary in the boundary regions, as k can easily (and erroneously) become negative in the zone of high gradients near the wall (due to overestimated dissipation), thus conflicting with the boundary condition (21). Computational procedure is also prone to divergence if the right choice of the initial values ($t = 0$) is not made. These unfortunate side effects become more and more severe as the Grashof number increases. In a real lake cross section the Grashof number can easily reach 10^{16} (due to a large width and relatively low kinematic viscosity of water), rendering the practical application of the k-ε closure model too complicated for seasonal hydrodynamic and water quality simulations of large lakes. In that regard, the k-ε model can still be recommended for relatively smaller physical domains (e.g. ponds and smaller reservoirs) and/or for the simulation of transient phenomena due to short-term external forcing (e.g. upwelling response of stratified water bodies to surface shear stress, excitation of baroclinic waves by variable wind fields in lakes, density currents). The aforementioned shortcomings of the k-ε model have led to consideration of another conventional closure scheme, popularly used in oceanography.

I.2.2. Mellor-Yamada (MY) Turbulence Closure Model

A hierarchy of turbulence closure models described by Mellor and Yamada (1974) has been in use in geophysical flows.. MY made use of the well-known approximations based on the hypotheses of Kolmogorof (1942), Prandtl (1945) and Rotta (1951) to simplify the exact transport equations for the Reynolds stress and the kinematic turbulent heat flux in the *Level 4* form

$$\frac{D}{Dt}\overline{u_i'u_j'} = \frac{\partial}{\partial x_k}\left[\frac{3}{5}lqS_q\left(\frac{\partial}{\partial x_k}\overline{u_i'u_j'} + \frac{\partial}{\partial x_j}\overline{u_i'u_k'} + \frac{\partial}{\partial x_i}\overline{u_j'u_k'}\right)\right] -$$

$$-\overline{u_k'u_i'}\frac{\partial \overline{u}_j}{\partial x_k} - \overline{u_k'u_j'}\frac{\partial \overline{u}_i}{\partial x_k} - \frac{2}{3}\frac{q^3}{\Lambda_1}\delta_{ij} - \frac{q}{3l_1}\left(\overline{u_i'u_j'} - \frac{\delta_{ij}}{3}q^2\right) + \qquad (22)$$

$$+ C_1 q^2\left(\frac{\partial \overline{u}_i}{\partial x_j} + \frac{\partial \overline{u}_j}{\partial x_i}\right) - \beta\left(g_j\overline{u_i'T'} + g_i\overline{u_j'T'}\right)$$

$$\frac{D}{Dt}\overline{u_i'T'} = \frac{\partial}{\partial x_k}\left[lqS_{uT}\left(\frac{\partial}{\partial x_k}\overline{u_i'T'} + \frac{\partial}{\partial x_i}\overline{u_k'T'}\right)\right] -$$

$$-\overline{u_i'u_k'}\frac{\partial \overline{T}}{\partial x_k} - \overline{u_k'T'}\frac{\partial \overline{u}_i}{\partial x_k} - \beta g_i \overline{T'^2} - \frac{q}{3l_2}\overline{u_i'T'} \tag{23}$$

$$\frac{D}{Dt}\overline{T'^2} = \frac{\partial}{\partial x_k}\left(lqS_T\frac{\partial}{\partial x_k}\overline{T'^2}\right) - 2\overline{u_k'T'}\frac{\partial \overline{T}}{\partial x_k} - 2\frac{q}{\Lambda_2}\overline{T'^2} \tag{24}$$

In the above equations β is the volumetric expansion coefficient, g_i is the gravitational acceleration, $q = \sqrt{\overline{u_i'u_i'}} = 2k$ is the turbulent kinetic energy. The length scales used in the model are all assumed proportional to a master length scale l, i.e.

$$(l_1, \Lambda_1, l_2, \Lambda_2) = (A_1, B_1, A_2, B_2)\, l \tag{25}$$

where $A_1 = 0.92, B_1 = 16.6, A_2 = 0.74$ and $B_2 = 10.1$ are fitted to experimental data.

The MY *Level 3* model is derived from the *Level 4* model using an order-of-magnitude analysis of small deviations of Reynolds stresses and heat flux $-\overline{u_i'T'}$ from the state of local isotropy (de facto neglecting the material derivatives and diffusion terms in (22) and (23))

$$\overline{u_i'u_j'} = \frac{\delta_{ij}}{3}q^2 - \frac{3l_1}{q}\left[\overline{u_k'u_i'}\frac{\partial \overline{u}_j}{\partial x_k} + \overline{u_k'u_j'}\frac{\partial \overline{u}_i}{\partial x_k} + \frac{2}{3}\delta_{ij}(P_s + P_b) - \right.$$

$$\left. - C_1 q^2\left(\frac{\partial \overline{u}_i}{\partial x_j} + \frac{\partial \overline{u}_j}{\partial x_i}\right) + \beta\left(g_j\overline{u_i'T'} + g_i\overline{u_j'T'}\right)\right] \tag{26}$$

$$\overline{u_i'T'} = -\frac{3l_2}{q}\left[\overline{u_i'u_k'}\frac{\partial \overline{T}}{\partial x_k} + \overline{u_k'T'}\frac{\partial \overline{u}_i}{\partial x_k} + \beta g_i \overline{T'^2}\right] \tag{27}$$

$$\frac{D}{Dt}\overline{T'^2} = \frac{\partial}{\partial x_k}\left(lqS_T\frac{\partial}{\partial x_k}\overline{T'^2}\right) - 2\overline{u_k'T'}\frac{\partial \overline{T}}{\partial x_k} - 2\frac{q}{\Lambda_2}\overline{T'^2} \tag{28}$$

where $P_s \equiv -\overline{u_i'u_j'}\frac{\partial \overline{u}_i}{\partial x_j}$ is the shear production and $P_b \equiv -\beta g_i \overline{u_i'T'}$ is the buoyant production of turbulent kinetic energy.

A further modification has been made to the *Level 3* model in terms of neglecting the material derivative and diffusion terms in Eq. (28)

$$\overline{T'^2} = -\frac{\Lambda_2}{q}\overline{u_k'T'}\frac{\partial \overline{T}}{\partial x_k} \tag{29}$$

This modification leads to the *Level 2½* closure model, which is frequently used in geophysical fluid dynamics problems. In addition to the algebraic expressions (26), (27) and (29), the *Level 2½* model utilizes the transport q-equation

$$\frac{Dq^2}{Dt} = \frac{\partial}{\partial x_k}\left(lqS_q \frac{\partial q^2}{\partial x_k} \right) + 2(P_s + P_b - \varepsilon) \tag{30}$$

which is the equivalent of the k-equation (11), previously used in the k-ε model. In the above equation $\varepsilon \equiv q^3/\Lambda_1$ is the dissipation of turbulent kinetic energy. Further modification of the *Level 2½* model leads to the fully algebraic *Level 2* model, which neglects the material derivative and diffusion terms in (29), stating that production of turbulent kinetic energy equals dissipation, $P_s + P_b = \varepsilon$. Because of its simplicity, the *Level 2* model is also widely used in practical applications.

For geophysical boundary layers, where horizontal gradients are much smaller than vertical ones, i.e. $\partial/\partial x$, $\partial/\partial y << \partial/\partial z$, the *Level 2½* model can be additionally simplified to

$$\frac{Dq^2}{Dt} = \frac{\partial}{\partial z}\left(lqS_q \frac{\partial q^2}{\partial z} \right) + 2(P_s + P_b - \varepsilon) \tag{31}$$

where $P_s = -\overline{u'w'}\frac{\partial \overline{u}}{\partial z} - \overline{v'w'}\frac{\partial \overline{v}}{\partial z}$, $P_b = \beta g \overline{w'T'}$. If it is further defined that

$$\begin{aligned} -\overline{u'w'} &= K_M \, \partial\overline{u}/\partial z \\ -\overline{v'w'} &= K_M \, \partial\overline{v}/\partial z \\ -\overline{T'w'} &= K_H \, \partial\overline{T}/\partial z \end{aligned} \tag{32}$$

where $K_M = lqS_M$ and $K_H = lqS_H$, then the *Level 2½* model boils down to a determination of coefficients S_M and S_H from the algebraic system (26)-(27). In the original model, these coefficients are solved as functions of $G_M = \frac{l^2}{q^2}\left[\left(\frac{\partial \overline{u}}{\partial z} \right)^2 + \left(\frac{\partial \overline{v}}{\partial z} \right)^2 \right]$ and $G_H \equiv -\frac{l^2}{q^2}\beta g \frac{\partial \overline{T}}{\partial z}$.

Galperin et al. (1988) proposed a quasi-equilibrium model where the coefficients are calculated as functions of only G_H (assuming local equilibrium $P_s + P_b = \varepsilon$), thus eliminating awkward realizability conditions (Hassid and Galperin 1983) related to dependence of the coefficients on velocity gradients. For the case of stable stratification ($\partial\overline{T}/\partial z > 0$), the lower bound $G_H \geq -0.28$ is suggested. In the case of unstable stratification ($\partial\overline{T}/\partial z < 0$), the upper bound $G_H \leq 0.0233$ is set. This model is more robust, while the principal advantage of the *Level 2½* model, namely the solution of a prognostic equation for turbulent kinetic energy (31), is retained.

The MY hierarchy of turbulence closure schemes requires also determination of the master length scale l (Eq. 25), to which all process scales are proportional. MY use an empirical master length scale equation

$$l = l_o \frac{\kappa z}{\kappa z + l_o}, \quad l_o = 0.1 \frac{\int_0^\infty |z| q dz}{\int_0^\infty q dz} \tag{33}$$

where $\kappa = 0.41$. For geophysical boundary layers this works well, but it is limited to boundary layers and does not have any general validity (e.g. for recirculating flows). For more general situations, MY also proposed a transport equation for $Z = q^2 l$, arguing that the application of the ε-transport equation (Eq. 12) is inappropriate for determining the required turbulent macroscale, as the dissipation ε describes the small-scale turbulence. However, the MY transport equation for the master length scale embodies some equally ambiguous terms for the application to recirculating flows.

It can be inferred that the major weakness of the MY turbulence closure model relates to the turbulent master length scale l, and, most important, to the fact that one sets all process scales proportional to a single scale. Although the model has been applied successfully to many geophysical problems in oceans and atmospheric boundary layers, its use for recirculating flows imposed by the boundaries of an enclosed body of water, such as a lake, is not justified. The use of two transport equations (for q and $q^2 l$) may improve the performance of the model in that respect, but would not remove the computational difficulties of the previous k-ε model. Therefore, the MY turbulence closure was not considered further.

I.3. LARGE EDDY SIMULATION (LES)

As was mentioned previously, an alternative for the description of turbulent flows is to work with *space* averages (rather than *time* averages) of the field variables and simulate their time history. Motions of scales smaller than the size of the space-averaging operator are characterized as subgrid scale (SGS) turbulence. Their effect on the development of the flow field is accounted for by using special closure models. This idea has led to the development of the Large Eddy Simulation method by Ferziger (Clark et al. 1979) and Reynolds (Kwak et al. 1975). A formal definition of the field variables used in LES provides the basis for a more complete formulation of the governing equations and a better understanding of the nature and functioning of the turbulence closure models used (Findikakis and Street 1982). Conventional turbulence closure models must account for the effect of turbulent motions extending over the entire range of possible scales in a given flow. SGS turbulence models, however, need to account for the effect of only a limited range of these scales, with an upper bound at the size of the averaging operator. This limited scope of the SGS turbulence closure models enhances their chances to succeed in different classes of flows because large-scale turbulence is in general flow dependent, while small-scale turbulence tends to be similar in most flows. This makes the use of space-averages for the description of turbulent flows particularly attractive for simulating geophysical flows.

The first step in this approach is to decompose each field variable ϕ into a large-scale (LS) component $\overline{\phi}$ and a SGS component ϕ'. The LS component can be defined using the convolution integral of ϕ with the Gaussian (or box) filter function (Findikakis and Street, 1982), but a simpler control-volume averaging is adopted in the present work

$$\overline{\phi} = \frac{1}{\Delta V} \int_V \phi dV \tag{34}$$

where ΔV is the size of the control volume. This approach facilitates the averaging of the nonlinear terms in the momentum and heat balance equations, using the simple form

$$\overline{\phi_i \phi_j} = \overline{\overline{\phi}_i \overline{\phi}_j} + \overline{\overline{\phi}_i \phi'_j} + \overline{\phi'_i \overline{\phi}_j} + \overline{\phi'_i \phi'_j} = \overline{\phi}_i \overline{\phi}_j + \overline{\phi'_i \phi'_j} \tag{35}$$

If the filter-function concept was used, the filtered value of the product $\overline{\phi}_i \overline{\phi}_j$ would not be equal to the product of the filtered components $\overline{\phi}_i \overline{\phi}_j$, neither would filtering the product of an LS component and an SGS component ($\overline{\overline{\phi}_i \phi'_j}$) give zero, since the filtered values are not constant in space. Instead, the additional terms would appear, and auxiliary approximations would be required (Clark 1979).

The use of control-volume averages formally enables the same set of governing equations for LS quantities (Eqs. 1-3) utilized previously for the description of the time-averaged flow variables, with the understanding that the overbars now imply space averaging. The difference is, however, in the treatment of fluctuating (SGS) components in these equations. The simplest available model for the SGS Reynolds stresses is the eddy viscosity approximation (4), rewritten here in the form

$$-\overline{u'_i u'_j} = 2\nu_t S_{ij} - \frac{2}{3} k \delta_{ij} \tag{36}$$

where $S_{ij} = \frac{1}{2}\left(\frac{\partial \overline{u}_i}{\partial x_j} + \frac{\partial \overline{u}_j}{\partial x_i} \right)$ is the LS rate of strain and $k = \frac{1}{2}\overline{u'_i u'_i}$ is the SGS turbulent kinetic energy per unit mass. An attempt to relate the eddy viscosity ν_t to the characteristics of the LS flow field and the size of the grid used for the numerical solution of the LS flow equations was made by Smagorinsky (1963), who proposed the following expression for the eddy viscosity

$$\nu_t = (c\Lambda)^2 S \tag{37}$$

where c is a constant, Λ is a characteristic length scale of SGS turbulence, related to the size of the largest eddies to be modeled by the LS equation, and $S = 2\sqrt{S_{ij} S_{ij}}$ is the total rate of strain. The constant c has been given values between 0.10 and 0.22 by different investigators. McMillan and Ferziger (1979), based on a number of computer tests, proposed the following expression for the constant c in terms of a SGS Reynolds number $R_{SGS} = \Lambda^2 S/\nu$

$$c = \frac{c_\infty}{1 + \frac{c_r}{R_{SGS}}} \tag{38}$$

where c_∞ is the value of c as $R_{SGS} \to \infty$. McMillan and Ferziger proposed $c_\infty = 0.176$ and $c_r = 18.8$.

The eddy viscosity expression (36) can be derived from the differential equations for the SGS Reynolds stresses and the SGS turbulent kinetic energy by making simplifying assumptions and closure approximations which involve only isotropic expressions for the approximated higher-order terms (Lilly 1967). In some simulations of turbulent flows in terms of space averages, the length scale Λ is equated to the cube root of the product of the typical finite difference cell dimensions. If the concept of the filter function is used, Λ is equal to the width of

the filter, which is not necessarily equal to the grid size. However, there is some uncertainty in using Smagorinsky's model for highly anisotropic grids (filters), which is unavoidable in simulations of many geophysical flows. Bardina et al. (1980) showed that when working with anisotropic grids, a more appropriate choice for the length scale of SGS turbulence is a scale proportional to the Euclidian norm of the dimensions of the typical grid cell. A special problem arises in near-wall regions, in which ν_t must be related to a characteristic length scale associated with near-wall turbulence. For two-dimensional simulations Schumann and Moin (1978) proposed the following expression near boundaries

$$\Lambda = \sqrt{\Delta_s \cdot \min(\Delta_n, \Lambda_n)} \tag{39}$$

where Δ_s is the grid size in the direction parallel to the boundary, Δ_n is its dimension normal to the boundary and Λ_n is a length scale associated with wall turbulence. For flows along solid surfaces good results are observed by using the van Driest damping function $\Lambda_n = 0.41y[1-\exp(-y^+/A^+)]$, where $y^+ = yu_*/\nu$, u_* is shear velocity, y is the distance from the wall and A^+ is usually evaluated as 26.

The simplest representation of turbulent transport in thermally nonuniform flows can be made by using Eq. (36) for the Reynolds stresses and by assuming that the turbulent flux of heat is proportional to the local temperature gradient, as expressed by Eq. (5). These equations may provide good approximation for the second-order SGS moments in cases where the production and redistribution by the LS field is isotropic. In stratified flows, however, these processes are not isotropic. Two possible alternative approaches for accounting for the stratification effect are (1) to use the eddy viscosity-eddy diffusivity model expressed by Eqs. (36) and (5) and modify empirically the expressions for the eddy coefficients; or (2) to solve the full differential equations for these quantities (as in the MY model). A third possibility, which goes beyond the empiricism of the first approach, but does not require the computational effort involved in the second approach, is to reduce the differential equations for the second-order moments to a system of algebraic equations that can then be solved to provide explicit expressions for the SGS Reynolds stresses and turbulent heat fluxes. Models of this type are referred to as algebraic SGS turbulence models.

By making a set of closure approximations in the differential equations for the SGS Reynolds stresses and turbulent heat fluxes, Findikakis and Street (FS 1979) were able to develop their algebraic model for SGS turbulence in stratified flow, assuming that SGS turbulence is in stationary equilibrium. The modified eddy viscosity is given by the following expression

$$\nu_t = f_S (c\Lambda)^2 \sqrt{2S_{ij}S_{ij}} \tag{40}$$

The stratification function f_S is evaluated from

$$f_S^2 = \frac{1-(q_1+q_2)\mathrm{Ri}+\sqrt{[1-(q_1+q_2)\mathrm{Ri}]^2+4q_2[\mathrm{Ri}+q_1(\mathrm{Ri}_{h1}^2+\mathrm{Ri}_{h2}^2)]}}{2} \tag{41}$$

where $\mathrm{Ri} = \frac{\beta g}{S^2}\frac{\partial \overline{T}}{\partial x_3}$ is the local Richardson number and $\mathrm{Ri}_{\mathrm{hk}} = \frac{\beta g}{S^2}\frac{\partial \overline{T}}{\partial x_{\mathrm{k}}}$ is a dimensionless measure of the horizontal temperature gradients defined only for the two horizontal directions, k = 1, 2. The solution for the horizontal turbulent heat fluxes can be set in the form of Eq. (5) with eddy diffusivity coefficients $\Gamma_{\mathrm{k}} = \nu_{\mathrm{t}}/\sigma_{\mathrm{t}}$, k = 1, 2. The vertical turbulent heat flux is

$$\overline{u_3' T'} = -f_{\mathrm{hj}} \frac{\nu_{\mathrm{t}}}{\sigma_{\mathrm{t}}} \frac{\partial \overline{T}}{\partial x_j} - f_{\mathrm{v}} \frac{\nu_{\mathrm{t}}}{\sigma_{\mathrm{t}}} \frac{\partial \overline{T}}{\partial x_3} \tag{42}$$

where $f_{\mathrm{v}} = \frac{1}{1 + q_2 \frac{\mathrm{Ri}}{f_{\mathrm{S}}^2}}$ and $f_{\mathrm{hj}} = -f_{\mathrm{v}} q_2 \beta g \frac{\partial \overline{T}/\partial x_j}{S^2}$. Coefficients q_1 and q_2 are evaluated at 2.5 and 2.94, respectively.

In a uniform-density flow ($\mathrm{Ri} = \mathrm{Ri}_{\mathrm{hk}} = 0$), Eq. (40) reduces to Smagorinsky's model. In a stratified shear flow where turbulent transport is totally suppressed when the local Richardson number exceeds a critical value, the model does not provide a satisfactory representation of turbulent transport. This is a weakness of the FS model, and can be overcome by using a more complete formulation of the SGS Reynolds stresses, resulting in more complex expressions for the eddy coefficients. In the present work a different approach is taken: the stratification function f_{S} is evaluated as (41) for unstable stratification ($\mathrm{Ri} < 0$), while for stable stratification ($\mathrm{Ri} > 0$), f_{S} is calculated from the correction factor $(1 + \beta R_i)^{\alpha}$ used in the empirical formula (6). Variation of the function f_{S} is shown in Fig. I-6 for $\mathrm{Ri}_{\mathrm{h}} = 0$, where the FS model is shown by the dotted line and the present approximation is given by the solid one. It can be seen how the FS model cannot totally suppress f_{S} in strong stratification, while the empirical formula (6) performs much better.

I.4. CONCLUSIONS

The two-equation differential turbulence model is often referred to as the simplest conventional closure for complex (recirculating) flows, because it accounts for the fact that both turbulence kinetic energy and dissipation are carried by the flow. This work confirms that the two-equation closure model is capable of capturing significant features of complex flow developments, relevant for lake applications. However, it was found that the numerical treatment of the two highly nonlinear, coupled transport equations in a high Grashof number flow (which is typical for larger lakes) suffers from restrictive stability criterion which considerably limits the computational time step. Special attention is also necessary in the boundary regions where the overestimated dissipation easily leads to computational divergence. In that regard, the two-equation (k-ε) turbulence model can only be recommended for relatively smaller physical domains (e.g. ponds and smaller reservoirs) and/or for the simulation of transient phenomena due to short-term external forcing.

The Mellor-Yamada (MY), one-equation differential turbulence closure model has been applied successfully to many geophysical problems in the ocean and atmospheric boundary layers. However, its use for complex recirculating flows, imposed by the boundaries of an

enclosed body of water (such as a lake), is not justified. The major weakness of the MY model relates to the turbulent master length scale l , and, most important, to the fact that one sets all process scales proportional to a single scale. The use of another transport equation for the length scale may improve the performance of the model in that respect, but would not remove the computational difficulties of the previous k-ε model.

The large-eddy-simulation approach, with modified algebraic (SGS) turbulence closure, was found in this work as a good alternative for lake hydrodynamic calculations. It is preferred over the differential, two-equation k-ε model for its simplicity and robustness, as well as over the one-equation MY model due to its consistency and more general applicability to different kinds of stratified flows. In order to completely evaluate the performance of this closure model for application in lakes, additional testing with experimental and field data would be recommended.

I.5. SECTION I. REFERENCES

Bardina, J., Ferziger, J. H., and Reynolds, W. C. (1980). "Improved subgrid-scale models for large-eddy simulation." *Paper No. 803157*, American Institute for Astronautics and Aeronautics.

Clark, R. A., Ferziger, J. H., and Reynolds, W. C. (1979). "Evaluation of sub-grid-scale turbulence models using an accurately simulated turbulent flow." *J. Fluid Mechanics*, vol. 91, No. 1, 1-16.

Findikakis, A. N., and Street, R. L. (1979). "An algebraic model for SGS turbulence in stratified flows." *J. Atmos. Sci.*, vol. 34, 923-934.

Findikakis, A. N., and Street, R. L. (1982). "Mathematical description of turbulent flows." *J. Hydr. Div.*, ASCE, vol. 108, No. HY8, 887-903.

Fraikin, M. P., Portier, J. J. and Fraikin, C. J. (1980). "Application of a k-ε turbulence model to an enclosed buoyancy driven recirculating flow." *J. Heat Transfer*, 80-HT-68, 1-12.

Galperin, B., Kantha, L. H., Hassid, S., and Rosati, A. (1988). "A quasi-equilibrium turbulent energy model for geophysical flows." *J. Atmos. Sci.*, vol. 45, No. 1, 55-62.

Hassid, S., and Galperin, B. (1983). "A turbulent energy model for geophysical flows." *Boundary-Layer Meteorology*, 26, 397-412.

Kolmogorof, A. N. (1942). *Equations of Turbulent Motion of an Incompressible Turbulent Fluid*, translated by D. B. Spalding, Imperial Coll. of Science and Techn., Dept. of Mech. Eng., ON/6, 1968.

Kwak, D. W., Reynolds, W. C., and Ferziger, J. H. (1975). "Three-dimensional time-dependent computation of turbulent flow." *Report TF-5*, Stanford University, Dept. of Mech. Eng.

Launder, B. E., and Spalding, D. B. (1974). "The numerical computation of turbulent flow." *Comp. Meth. Appl. Mech. Eng.*, 3, 269-289.

Lilly, D. K. (1967). "The representation of small-scale turbulence in numerical simulation experiments." *Proceedings of the IBM Scientific Symposium on Environmental Sciences*, 195-210.

McMillan, O. J., and Ferziger, J. H. (1979). "Direct testing of sub-grid-scale models.", *Paper 79-0072*, presented at the 17th Aerospace Sciences Meeting, New Orleans.

Mellor, G. L., and Yamada, T. (1974). "A hierarchy of turbulence closure models for planetary boundary layers." *J. Atmos. Sci.*, 31, 1791-1806.

Moin, P., Reynolds, W. C., and Ferziger, J. H. (1978). "Large eddy simulation of incompressible channel flow." *Report TF-12*, Stanford University, Dept. Mech. Eng.

Munk, W. H., and Anderson, E. R. (1948). "Notes on the theory of the thermocline." *J. Marine Research*, vol. 1.

Papanicolaou, E, and Jaluria, Y. (1995). "Computation of turbulent flow in mixed convection in a cavity with a localized heat source." *J. Heat Transfer*, 117, 649-658.

Prandtl, L. (1945). *Über ein neues Formellsystem für die ausgebildete Turbulenz*, Nachr. Akad. Wiss. Got., Math-Phys. Klasse, No. 6.

Rodi, W. (1980). *Turbulence Models and Their Application In Hydraulics-a State-of-the-Art Review*. International Association of Hydraulic Research, Delft, The Netherlands.

Rotta, J. C. (1951). "Statistiche theorie nichthomogener turbulenz." *Z. Physik*, 129, 547-572.

Schumann, U. (1974). "Subgrid scale model for finite difference simulations of turbulent flows in plane channels and annuli." *J. Comp. Physics*, vol. 18, 376-404.

Smagorinsky, J. (1963). *General Circulation Experiments with the Primitive Equations:I-The Basic Experiment.*

Stefanovic, D. L. and Stefan, H. G. (1999). "Simulation of transient cavity flows driven by buoyancy and shear." *J. Hydr. Research*, in print.

Turner, J. S. (1973). *Buoyancy Effects in Fluids*, Cambridge University Press.

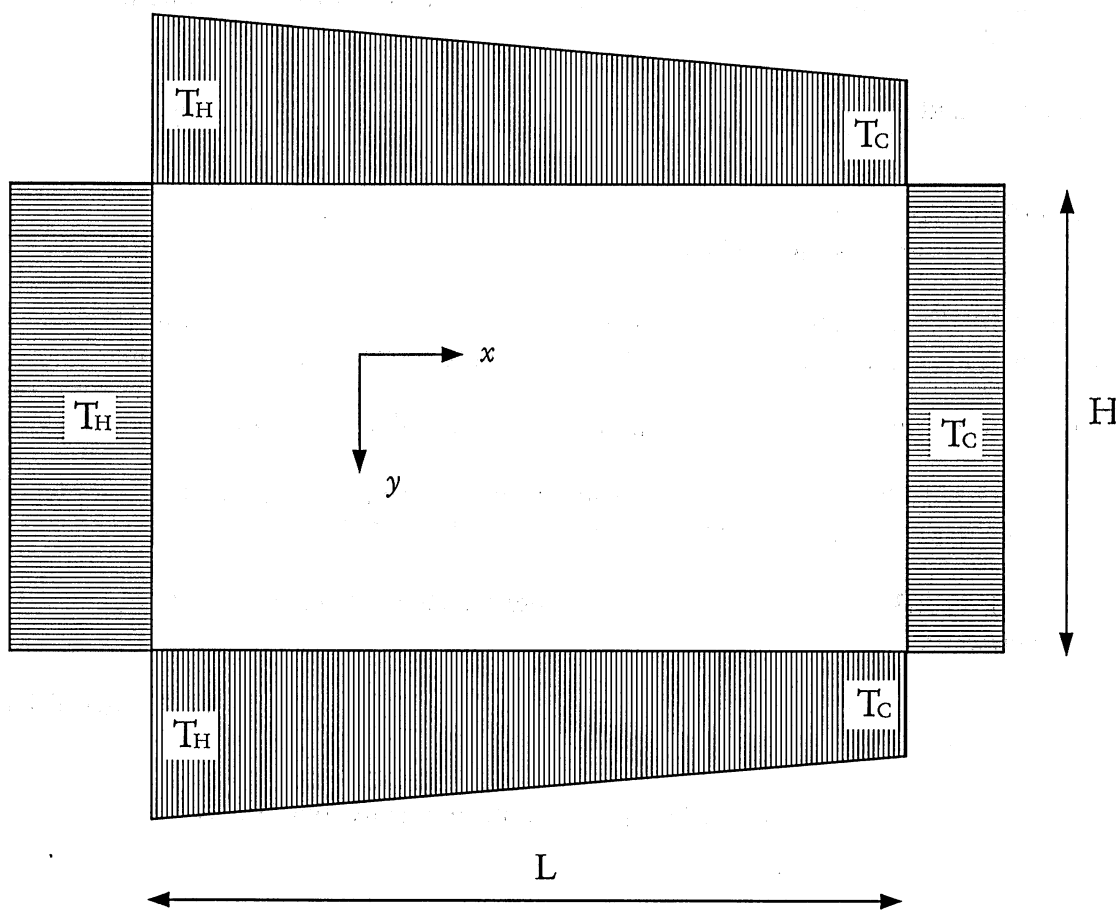

Figure I-1. Rectangular cavity domain.

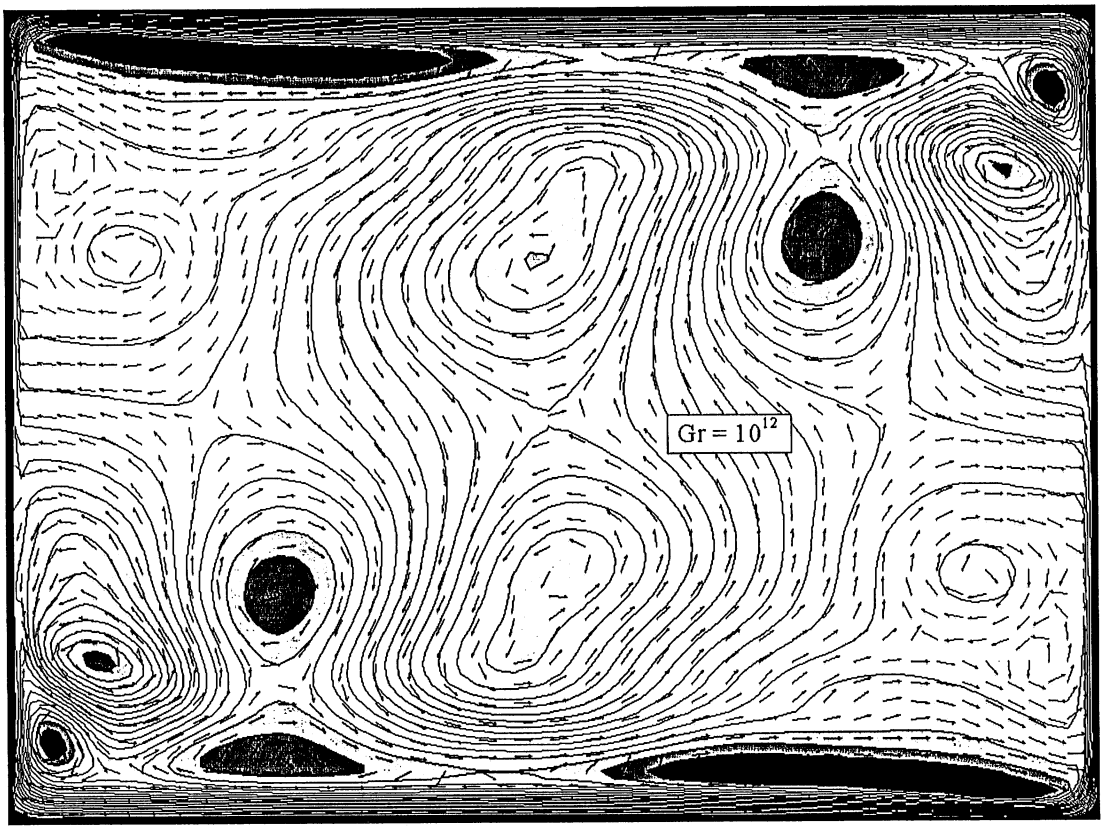

Figure I-2. Typical transient flow field for high Grashof numbers.

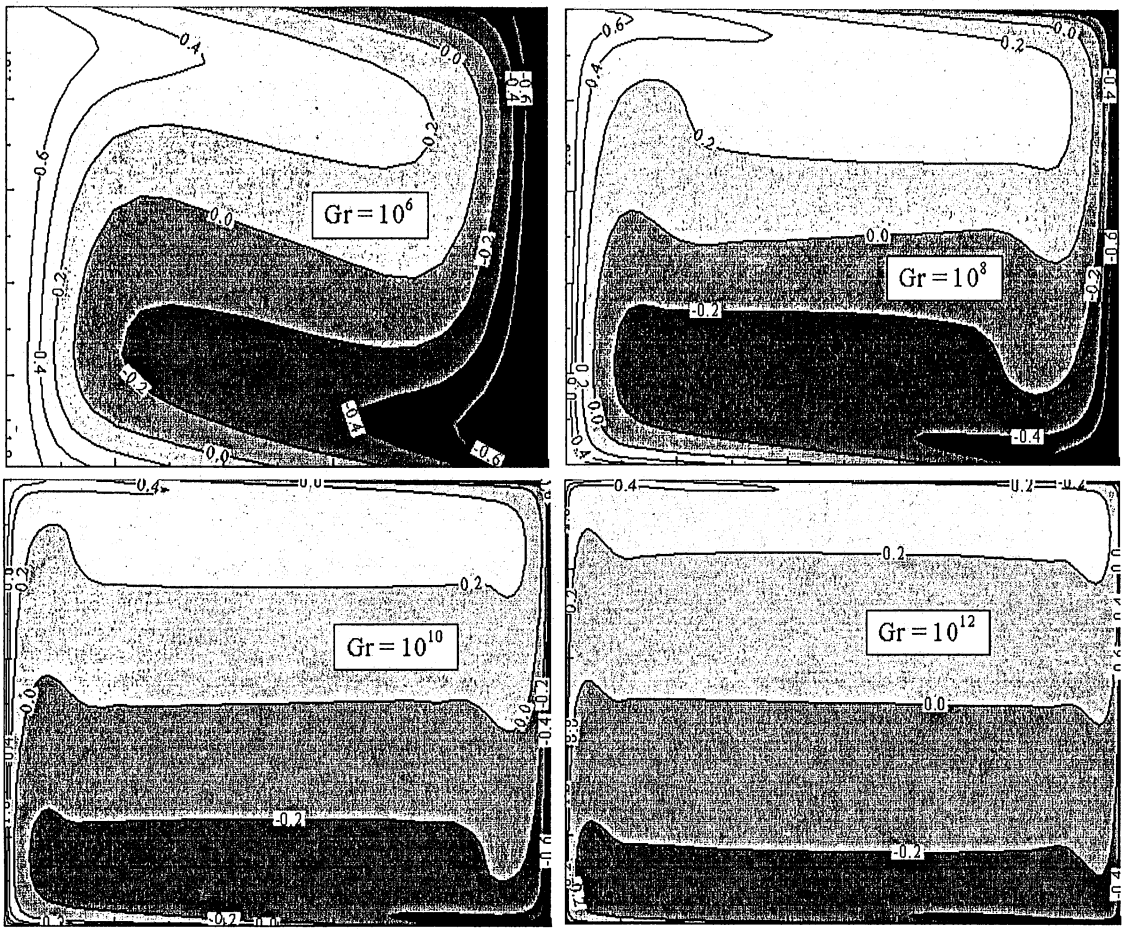

Figure I-3. Dimensionless temperature.

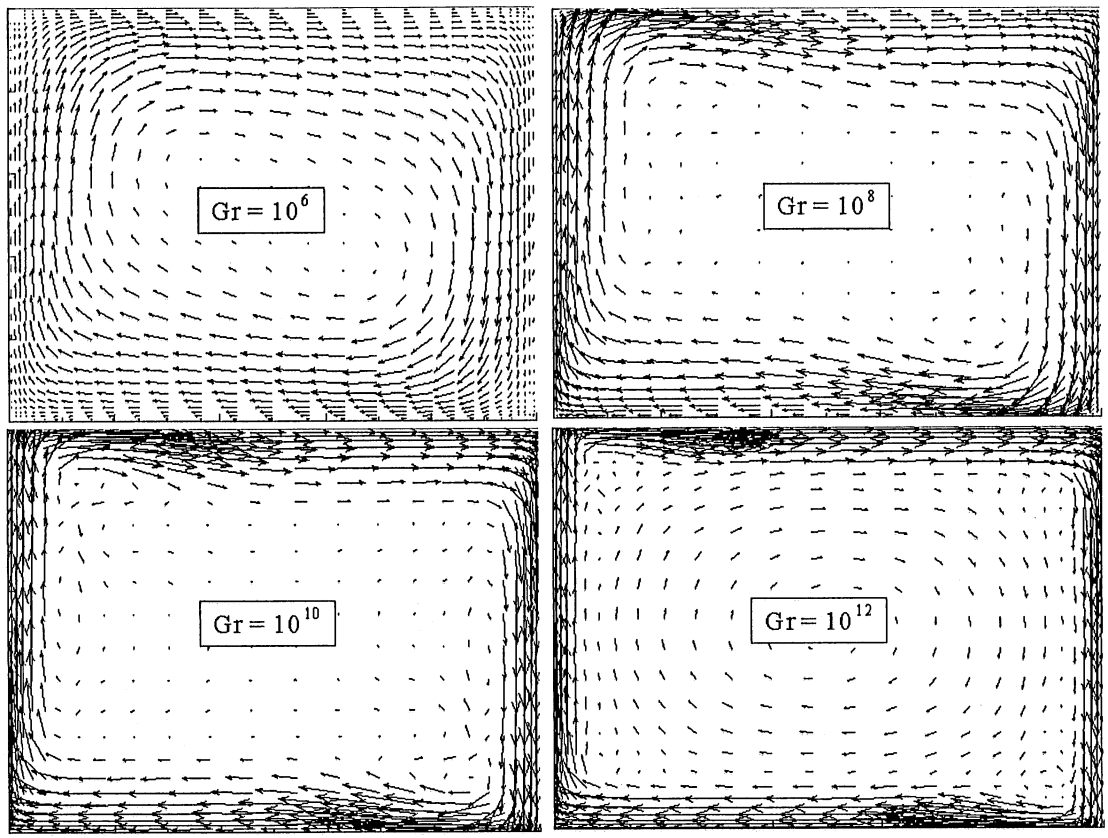

Figure I-4. Velocity vectors.

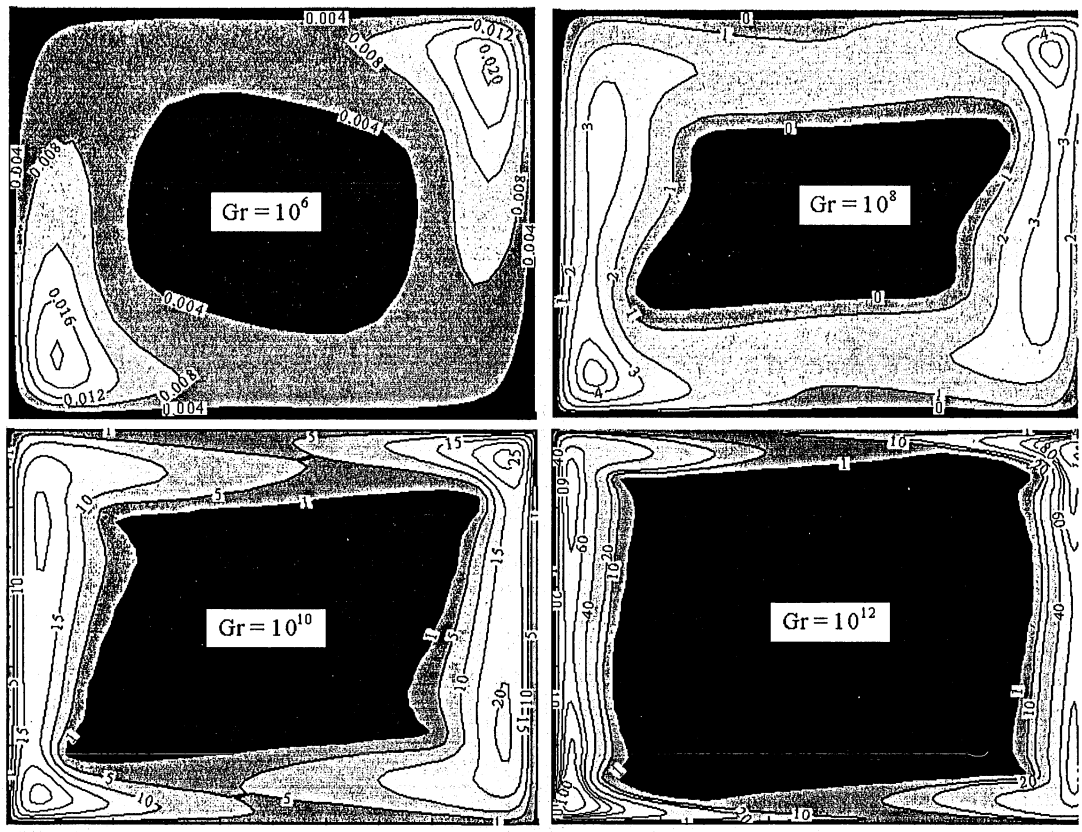

Figure I-5. Dimensionless eddy viscosity.

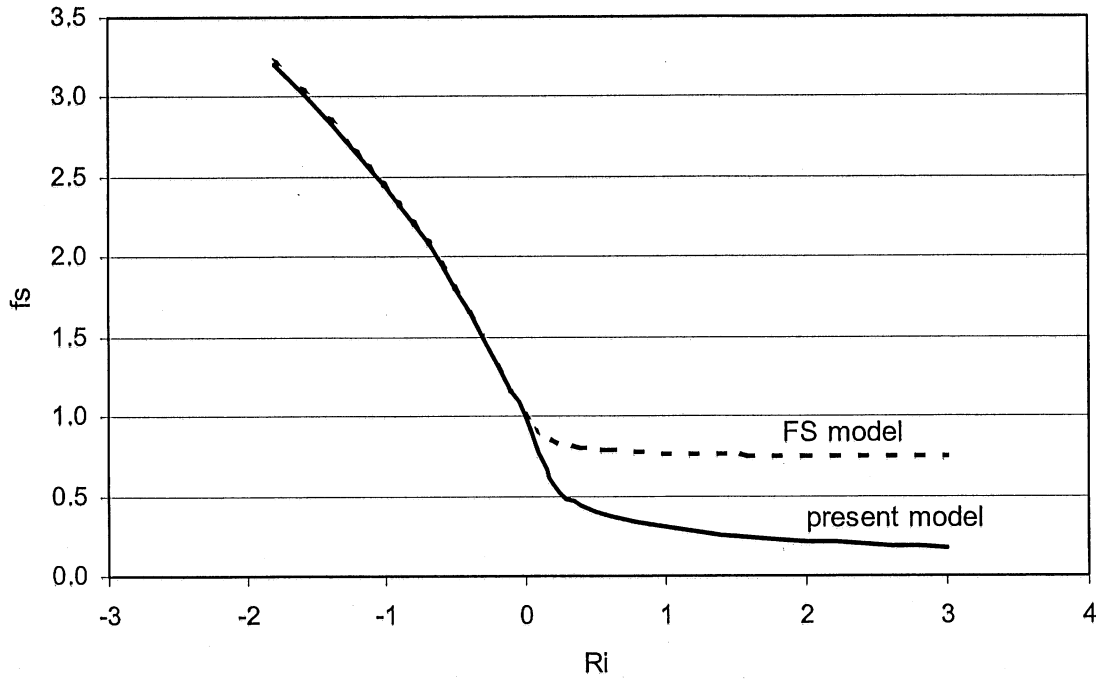

Figure I-6. Stratification function $f_S(\mathrm{Ri})$ for $\mathrm{Ri}_{hk} = 0$.

II. TRANSFORMATION OF THE PHYSICAL DOMAIN INTO A COMPUTATIONAL DOMAIN WITH APPLICATION TO LAKE MODELING

II.1. INTRODUCTION

Finite difference equations in two dimensions are most efficiently solved in a rectangular domain (Hoffmann and Chiang 1993). Unfortunately, the majority of physical domains encountered are nonrectangular in shape. For instance, lake cross sections considered in this work can be of arbitrary shape, making it desirable to transform the nonrectangular physical domain to a rectangular computational domain. It is also important to note that the transformation allows the alignment of one of the coordinates along a physical boundary, thus facilitating the implementation of the boundary conditions. The objective of the transformation (mapping, grid generation) is then to identify the location of the grid points in the computational domain and the location of the corresponding grid points in the physical space. However, the resulting system of transformed governing equations is more complicated than the original one. Thus, a trade-off is introduced whereby advantages gained by using the generalized coordinates are somehow counterbalanced by the resultant intricacy of the transformed system. Fortunately, the advantages by far outweigh the complexity of the procedure (Hoffmann and Chiang 1993).

II.2. COORDINATE TRANSFORMATION

The process of transformation of a typical 2-D partial differential equation is illustrated below. The following relations (mapping) between the physical (x, y) and computational space (ξ, η) are assumed

$$\xi = \xi(x, y), \quad \eta = \eta(x, y) \tag{43}$$

The chain rule for partial differentiation yields

$$\frac{\partial}{\partial x} = \frac{\partial \xi}{\partial x}\frac{\partial}{\partial \xi} + \frac{\partial \eta}{\partial x}\frac{\partial}{\partial \eta}, \quad \frac{\partial}{\partial y} = \frac{\partial \xi}{\partial y}\frac{\partial}{\partial \xi} + \frac{\partial \eta}{\partial y}\frac{\partial}{\partial \eta} \tag{44}$$

where $\xi_x = \partial\xi/\partial x$, $\eta_x = \partial\eta/\partial x$, $\xi_y = \partial\xi/\partial y$ and $\eta_y = \partial\eta/\partial y$ are defined as the metrics of transformation or simply as the metrics. They represent the ratio of arc lengths in the computational space to that of the physical space.

Also, from mapping (43), the following differential expressions are obtained

$$d\xi = \xi_x dx + \xi_y dy, \quad d\eta = \eta_x dx + \eta_y dy \tag{45}$$

which are written in a compact form as

$$\begin{bmatrix} d\xi \\ d\eta \end{bmatrix} = \begin{bmatrix} \xi_x & \xi_y \\ \eta_x & \eta_y \end{bmatrix} \begin{bmatrix} dx \\ dy \end{bmatrix} \tag{46}$$

Reversing the role of independent variables, i.e.

$$x = x(\xi,\eta), \quad y = y(\xi,\eta) \tag{47}$$

the following may be written

$$\begin{bmatrix} dx \\ dy \end{bmatrix} = \begin{bmatrix} x_\xi & x_\eta \\ y_\xi & y_\eta \end{bmatrix} \begin{bmatrix} d\xi \\ d\eta \end{bmatrix} \tag{48}$$

Comparing Eqs. (46) and (48), it can be concluded that

$$\begin{bmatrix} \xi_x & \xi_y \\ \eta_x & \eta_y \end{bmatrix} = \begin{bmatrix} x_\xi & x_\eta \\ y_\xi & y_\eta \end{bmatrix}^{-1} \tag{49}$$

from which follows

$$\begin{aligned} \xi_x &= J\, y_\eta \\ \xi_y &= -J x_\eta \\ \eta_x &= -J\, y_\xi \\ \eta_y &= J x_\xi \end{aligned} \tag{50}$$

where $J = 1/(x_\xi\, y_\eta - y_\xi x_\eta)$ is defined as the Jacobian of transformation, representing the ratio of the areas (volumes in 3-D) in the computational space to that in the physical space.

Now consider a model partial differential equation (PDE) in the conservative form

$$\frac{\partial \phi}{\partial t} + \frac{\partial u\phi}{\partial x} + \frac{\partial v\phi}{\partial y} = \frac{\partial}{\partial x}\left(\alpha_x \frac{\partial \phi}{\partial x}\right) + \frac{\partial}{\partial y}\left(\alpha_y \frac{\partial \phi}{\partial y}\right) + S \tag{51}$$

This equation may be transformed from physical space to computational space using Eqs. (44). The result will be shown first for the left-hand side (LHS) of Eq. (51)

$$\text{LHS} = \frac{\partial \phi}{\partial t} + \xi_x \frac{\partial u\phi}{\partial \xi} + \eta_x \frac{\partial u\phi}{\partial \eta} + \xi_y \frac{\partial v\phi}{\partial \xi} + \eta_y \frac{\partial v\phi}{\partial \eta} \tag{52}$$

It is recognized that this equation is no longer in a conservative form. To recast it in a desirable conservative form, some manipulation must be performed. For that reason, Eq. (52) is divided by J and a combination of terms (which sum up to zero) is added to give

$$\text{LHS}=\frac{1}{J}\frac{\partial\phi}{\partial t}+\frac{\xi_x}{J}\frac{\partial u\phi}{\partial\xi}+u\phi\frac{\partial}{\partial\xi}\left(\frac{\xi_x}{J}\right)+\frac{\eta_x}{J}\frac{\partial u\phi}{\partial\eta}+u\phi\frac{\partial}{\partial\eta}\left(\frac{\eta_x}{J}\right)+\frac{\xi_y}{J}\frac{\partial v\phi}{\partial\xi}+v\phi\frac{\partial}{\partial\xi}\left(\frac{\xi_y}{J}\right)+$$
$$+\frac{\eta_y}{J}\frac{\partial v\phi}{\partial\eta}+v\phi\frac{\partial}{\partial\eta}\left(\frac{\eta_y}{J}\right)-u\phi\left[\frac{\partial}{\partial\xi}\left(\frac{\xi_x}{J}\right)+\frac{\partial}{\partial\eta}\left(\frac{\eta_x}{J}\right)\right]-v\phi\left[\frac{\partial}{\partial\xi}\left(\frac{\xi_y}{J}\right)+\frac{\partial}{\partial\eta}\left(\frac{\eta_y}{J}\right)\right] \tag{53}$$

According to (50), the last two terms in the above equation are zero, yielding the equivalent conservative form of Eq. (52)

$$\text{LHS}=\frac{\partial}{\partial t}\left(\frac{\phi}{J}\right)+\frac{\partial}{\partial\xi}\left(\xi_x\frac{u\phi}{J}+\xi_y\frac{v\phi}{J}\right)+\frac{\partial}{\partial\eta}\left(\eta_x\frac{u\phi}{J}+\eta_y\frac{v\phi}{J}\right) \tag{54}$$

Extending this conclusion to the right-hand side of Eq. (51) results in the following transformed equation

$$\frac{\partial}{\partial t}\left(\frac{\phi}{J}\right)+\frac{\partial}{\partial\xi}\left(\xi_x\frac{u\phi}{J}+\xi_y\frac{v\phi}{J}\right)+\frac{\partial}{\partial\eta}\left(\eta_x\frac{u\phi}{J}+\eta_y\frac{v\phi}{J}\right)=\frac{\partial}{\partial\xi}\left(\frac{\xi_x^2\alpha_x+\xi_y^2\alpha_y}{J}\frac{\partial\phi}{\partial\xi}\right)+$$
$$\frac{\partial}{\partial\xi}\left(\frac{\xi_x\eta_x\alpha_x+\xi_y\eta_y\alpha_y}{J}\frac{\partial\phi}{\partial\eta}\right)+\frac{\partial}{\partial\eta}\left(\frac{\xi_x\eta_x\alpha_x+\xi_y\eta_y\alpha_y}{J}\frac{\partial\phi}{\partial\xi}\right)+ \tag{55}$$
$$\frac{\partial}{\partial\eta}\left(\frac{\eta_x^2\alpha_x+\eta_y^2\alpha_y}{J}\frac{\partial\phi}{\partial\eta}\right)+\frac{S}{J}$$

It is obvious that the PDE (55) is more complex than the original equation (51), but the advantages of the mapping procedure as a whole outweigh these complications.

Several requirements must be placed on the mapping of the physical domain to the computational domain. A partial list can be stated as follows (Tannehill et al. 1997):

- the mapping must be one to one (grid lines of the same family do not cross each other)
- the grid lines should be smooth to provide continuous transformation derivatives
- grid points should be closely spaced in the physical domain where large gradients (numerical errors) are expected
- excessive grid skewness should be avoided. It has been shown (Raithby 1976) that grid skewness sometimes exaggerates truncation errors.

In general, grid generation techniques may be roughly classified as (1) algebraic methods, (2) partial differential equation (PDE) methods, or (3) conformal mappings based on complex variables. The last approach is limited to 2-D problems and requires a reasonable knowledge of complex variables. In addition, the determination of the mapping function is sometimes a difficult task. Therefore, the first two methods for generating computational grids

show the most promise for continued development and use in conjunction with finite-difference methods (Tannehill et al. 1997).

The simplest grid generation technique is the algebraic method. An algebraic equation is used to relate the grid points in the computational domain to those of the physical domain. This objective is met by using an interpolation scheme between the specified boundary grid points to generate the interior grid points. The major advantages of this approach are: the speed with which a grid can be generated; metrics may be evaluated analytically, thus avoiding numerical errors; the ability to cluster grid points in different regions can be easily implemented. The disadvantages are: discontinuities at a boundary may propagate into the interior region which could lead to errors due to sudden changes in the metrics; control of grid smoothness and skewness is a difficult task.

Some of the disadvantages of the algebraic grid generators are overcome by the use of PDE methods which is, of course, accomplished with increased computational time. In these methods, a system of PDEs is solved for the location of the grid points in the physical space, whereas the computational domain is a rectangular shape with uniform grid spacing.

II.2.1. Algebraic Grid Generation

In this work a simple, but very effective algebraic mapping was devised, with a special care paid to avoid the aforementioned disadvantages of the approach.

Consider the simple physical domain depicted in Fig. II-1. Introducing the following algebraic relations will transform this nonrectangular physical domain into a rectangular one

$$0<\xi=x<L,\ 0<\eta=\frac{y}{H_1+\frac{H_2-H_1}{L}x}<1.0 \tag{56}$$

The following transformation metrics result from the mapping (56)

$$\begin{aligned}\xi_x &= 1\\ \xi_y &= 0\\ \eta_x &= -J\frac{H_2-H_1}{L}\eta\\ \eta_y &= J\end{aligned} \tag{57}$$

where the Jacobian of transformation is given as

$$J=\frac{1}{H_1+\frac{H_2-H_1}{L}\xi} \tag{58}$$

The grid system is generated as follows. The geometry in the physical space is defined by specifying values of L, H_1 and H_2. Next, the desired number of grid points in the horizontal direction (*nx*) and vertical direction (*ny*) is set. The uniform grid lines in the computational domain (Fig. II-2) are produced at distances $\Delta\xi = L/(nx\text{-}1)$ and $\Delta\eta = 1.0/(ny\text{-}1)$. Once the computational domain is constructed , the values of ξ and η are known at each grid point within

the domain. Also, the governing PDE of the form (55) can be solved when the metrics (57) are evaluated in the transformed coordinate system. Finally, the reverse mapping

$$x = \xi, \quad y = \left(H_1 + \frac{H_2 - H_1}{L} \xi \right) \eta \tag{59}$$

is employed to identify the corresponding grid points in the physical space.

The algebraic mapping described above for a simple physical domain depicted in Fig. II-1 is used as a building block for more complex physical domains, i.e. lake cross sections. A lake cross section is assumed to be composed of several trapezoidal segments (Fig. II-3) and the foregoing transformation is applied to each particular segment i defined by its L^i, $H_1{}^i$ and $H_2{}^i$. An irregular physical domain is thus transformed into rectangular computational domain shown in Fig. (II-4). This is possible because η (Eq. 56) is normalized for each segment, i.e. its value always ranges from zero to one.

Special attention is necessary along the adjoining sides of the neighboring segments, due to discontinuity in the metric η_x (Eq. 57). Therefore, η_x is evaluated along the adjacent sides as the arithmetic average of the corresponding values for the left and right segment. It should also be noted that neither $H_1{}^i$ nor $H_2{}^i$ are allowed to vanish, as the Jacobian (Eq. 58) would become infinite at the corresponding end of the segment. This is important for the first and last segment of a lake cross section (Fig. II-3), where some arbitrary small endpoint depths (e.g. 5% of the maximum lake depth) must be specified. The previous warrants smooth distribution of the transformation metrics, which is a necessary condition for proper mapping procedure. As was discussed earlier, it is also recommended to avoid excessive grid skewness. This condition is naturally satisfied for shallow lakes that often tend to have the aspect ratios (depth/width) less than 0.05.

For flow problems where large gradients are concentrated in a specific region, additional resolution of the flow properties is essential. These regions are regularly found near the physical boundaries of the flow. For the mixed convection problems in lakes, where the flows are driven by combined wind shear and thermal effects, it is necessary to use finer grids near the water surface and close to the lake bottom (to capture properly both velocity and temperature gradients). Rather than using a uniform grid distribution described previously, grid points may be clustered in the regions of high gradients, which reduces the total number of computational points and thus increases efficiency. The clustering used in this work is based on the Papanicolaou and Jaluria (1995) hyperbolic grid

$$\eta_j = 0.5 \left\{ 1 + \frac{\tanh\left[a \left(\frac{j-1}{ny-1} - 0.5 \right) \right]}{\tanh\left(\frac{a}{2} \right)} \right\}, \quad j = 1, \ldots, ny \tag{60}$$

where ny is the total number of grid points j in the vertical direction and the best choice for constant a was found to be 4.0. This technique gradually increases the grid spacing from the

horizontal walls towards the interior of the domain (Fig. II-5), providing high accuracy without severe reduction of the allowable time step.

II.3. BOUNDARY CONDITIONS IN THE COMPUTATIONAL DOMAIN

The algebraic mapping (56) transforms the arbitrarily shaped bottom boundary of the physical domain (Fig. II-3) into the straight boundary line, $\eta = 1.0$, of the computational domain (Fig. II-4). Other boundaries are transformed in a like manner. Consequently, the transformation of the physical domain into a rectangular computational domain facilitates substantially the implementation of the boundary conditions. These conditions in the computational domain (Fig. II-4) are discussed below for each particular model variable.

II.3.1. Velocity Components (u, v)

The usual no-slip condition, $u = v = 0$, is used on solid boundaries ($\xi = 0$, $\xi = L$, $\eta = 1.0$). At the water surface ($\eta = 0.0$), the wind-shear boundary condition is specified, while the u-component velocity is subsequently calculated from the stream function distribution ($u = J\,\partial\psi/\partial\eta$). The v-component velocity is set at zero, neglecting the rate of change of water elevation due to surface waves. This approximation is justifiable for regular wind events and will not significantly influence the overall circulation pattern in a lake cross section.

II.3.2. Stream Function (ψ)

Along the boundaries of the physical domain it holds

$$d\psi \equiv \frac{\partial\psi}{\partial x}dx + \frac{\partial\psi}{\partial y}dy = -vdx + udy = 0 \tag{61}$$

Thus, for a closed physical contour (without inflows/outflows) it follows that the stream function ψ is equal to constant (=0). As the boundaries of the physical domain are mapped on the boundaries of the computational domain, the constant ψ function condition also applies in the computational domain.

II.3.3. Vorticity (ϖ)

The boundary conditions for the vorticity do not exist and must be constructed using the stream function equation, along with Taylor series expansion of the stream function (Stefanovic and Stefan 1999). The Poisson equation for the stream function in the physical domain

$$\frac{\partial^2\psi}{\partial x^2} + \frac{\partial^2\psi}{\partial y^2} = -\varpi \tag{62}$$

is transformed in the computational domain to yield

$$\frac{\partial}{\partial\xi}\left(\frac{\xi_x^2+\xi_y^2}{J}\frac{\partial\psi}{\partial\xi}\right)+\frac{\partial}{\partial\xi}\left(\frac{\xi_x\eta_x+\xi_y\eta_y}{J}\frac{\partial\psi}{\partial\eta}\right)+\frac{\partial}{\partial\eta}\left(\frac{\xi_x\eta_x+\xi_y\eta_y}{J}\frac{\partial\psi}{\partial\xi}\right)+$$
$$\frac{\partial}{\partial\eta}\left(\frac{\eta_x^2+\eta_y^2}{J}\frac{\partial\psi}{\partial\eta}\right)=-\frac{\omega}{J} \tag{63}$$

Equation (63) can be greatly simplified on the walls using the velocity boundary conditions.

Along the vertical walls ($\xi = 0$ and $\xi = L$), both velocity components are zero, i.e.

$$u\equiv\frac{\partial\psi}{\partial y}=\frac{\partial\psi}{\partial\xi}\xi_y+\frac{\partial\psi}{\partial\eta}\eta_y=\frac{\partial\psi}{\partial\eta}J=0 \tag{64}$$

$$v\equiv-\frac{\partial\psi}{\partial x}=-\frac{\partial\psi}{\partial\xi}\xi_x-\frac{\partial\psi}{\partial\eta}\eta_x=-\frac{\partial\psi}{\partial\xi}-\frac{\partial\psi}{\partial\eta}\eta_x=0 \tag{65}$$

resulting in zero stream function gradients

$$\frac{\partial\psi}{\partial\xi}=\frac{\partial\psi}{\partial\eta}=0 \tag{66}$$

By the use of the previous condition and the metrics (57), Eq. (63) is simplified as follows

$$\frac{\partial}{\partial\xi}\left(\frac{1}{J}\frac{\partial\psi}{\partial\xi}\right)=-\frac{\omega}{J} \tag{67}$$

which gives the vorticity boundary condition on the vertical walls

$$\omega(\xi=0,\,L;\eta)=-\frac{\partial^2\psi}{\partial\xi^2} \tag{68}$$

The second derivative of ψ is further expended using the stream function values from the interior points of the computational domain, as described in Stefanovic and Stefan (1999).

The condition (66) is also applicable at the horizontal bottom wall ($\eta = 1.0$), resulting in the following simplification of Eq. (63)

$$\frac{\partial}{\partial\eta}\left(\frac{\eta_x^2+J^2}{J}\frac{\partial\psi}{\partial\eta}\right)=-\frac{\omega}{J} \tag{69}$$

The vorticity boundary condition on the bottom wall is then calculated as follows

$$\omega(\xi,\eta=1.0)=-\left(\eta_x^2+J^2\right)\frac{\partial^2\psi}{\partial\eta^2} \tag{70}$$

On the water surface ($\eta = 0.0$), the condition (70) still holds, but will result in different vorticity boundary condition, as the u-component velocity is not zero there. The second derivative of ψ is now evaluated from the wind shear τ, in the following form

$$\frac{\partial^2 \psi}{\partial \eta^2} = \frac{\tau}{\mu J^2} \tag{71}$$

where μ is the dynamic viscosity of water. The previous combined with Eq. (70) describes the vorticity on the water surface as

$$\omega(\xi, \eta = 0.0) = -\frac{\tau}{\mu} \tag{72}$$

II.3.4. Heat Flux (q_H^t)

Solar radiation flux q_H is supplied as the boundary condition on the water surface. When the transformation of the physical domain in a computational domain takes place, this flux has to be transformed as well. Heat flux is proportional to the temperature gradient, i.e.

$$q_H = \alpha \frac{\partial T}{\partial y} = \alpha \frac{\partial T}{\partial \eta} J \tag{73}$$

Therefore, the transformed heat flux at $\eta = 0.0$, proportional to the temperature gradient in the computational domain, is calculated as

$$q_H^t = \frac{q_H}{J} \tag{74}$$

II.3.5. Dissolved Oxygen Flux (q_O^t)

There are two dissolved oxygen boundary fluxes relevant for this study: aeration flux on the water surface and sedimentary oxygen flux at the lake bottom. These fluxes are transformed in the same manner as heat flux, because they are proportional to the gradient of dissolved oxygen concentration. Thus, the following transformation results

$$q_O^t = \frac{q_O}{J} \tag{75}$$

where q_O is oxygen flux in the physical domain.

II.4 CONCLUSIONS

In this section a simple and computationally efficient coordinate transformation, i.e. the mapping of the physical domain into a computational domain, is described. A lake cross section is assumed to be composed of several trapezoidal segments and the algebraic mapping function is applied to each particular segment, transforming an irregular physical domain into rectangular computational domain. This technique allows more efficient computational algorithm for the

solution of governing flow and transport equations and considerably facilitates the implementation of the boundary conditions.

II.5. SECTION II - REFERENCES

Tannehill, J. C., Anderson, D. A., and Pletcher R.H. (1997). *Computational Fluid Mechanics and Heat Transfer*, Taylor & Francis, Washington, DC.

Papanicolaou, E, and Jaluria, Y. (1995). "Computation of turbulent flow in mixed convection in a cavity with a localized heat source." *J. Heat Transfer*, 117, 649-658.

Hoffmann, K. A., and Chiang, S. T. (1993). *Computational Fluid Mechanics for Engineers*, Vol. 1, Engineering Educational System, Wichita, Kansas.

Stefanovic, D. L. & Stefan, H. G. (1999). "Simulation of transient cavity flows driven by buoyancy and shear." *J. Hydr. Research*, in print.

Raithby, G. D. (1976). "Skew upstream differencing schemes for problems involving fluid flow." *Comput. Methods Appl. Mech. Eng.*, vol. 9, 153-164.

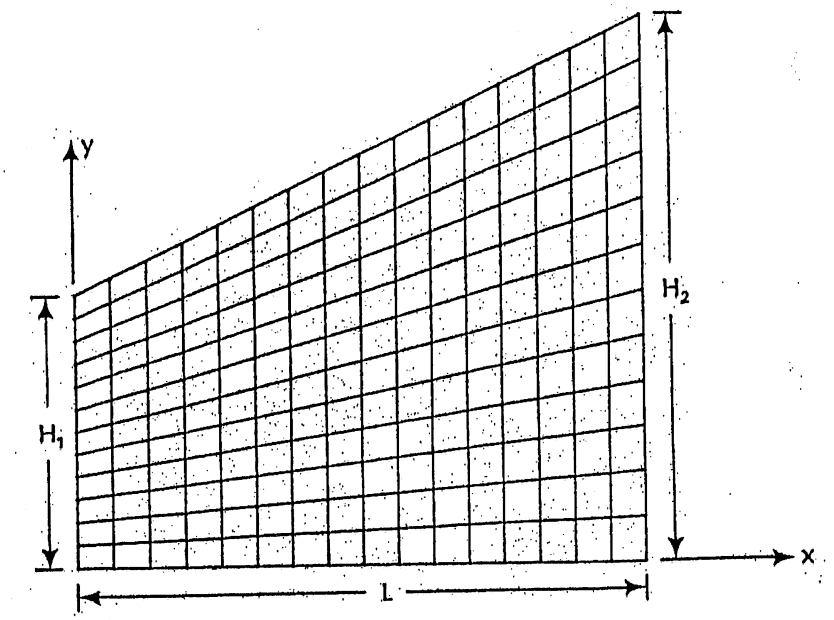

Figure II-1. Nonrectangular physical domain.

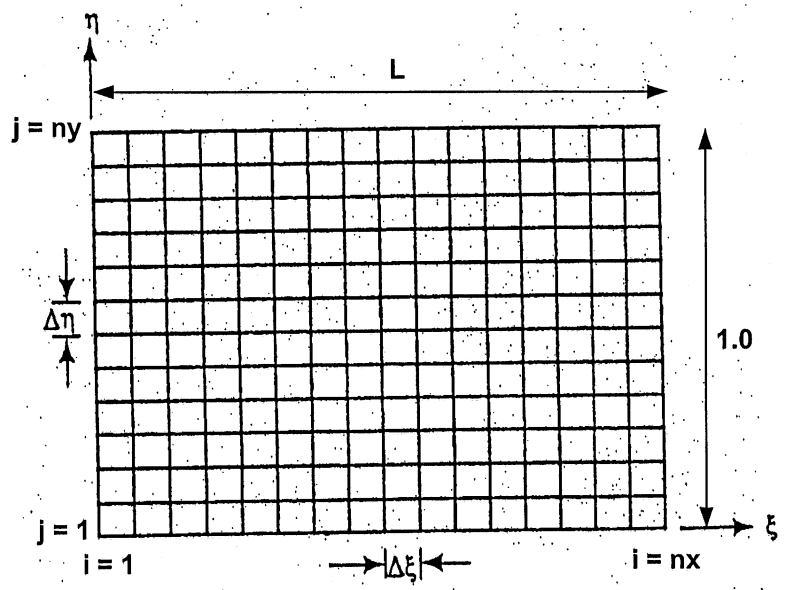

Figure II-2. Rectangular computational domain.

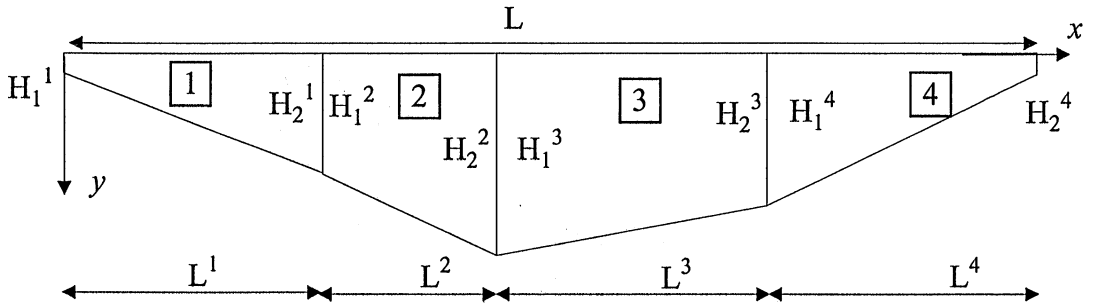

Figure II-3. Lake cross section divided into segments.

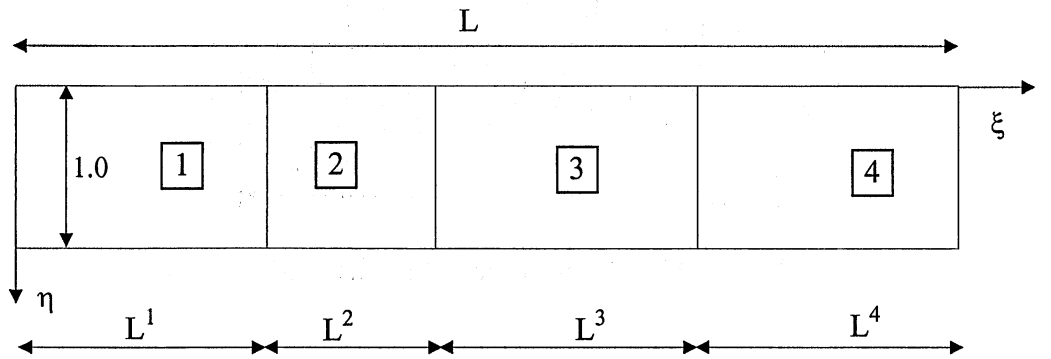

Figure II-4. Transformed lake cross section.

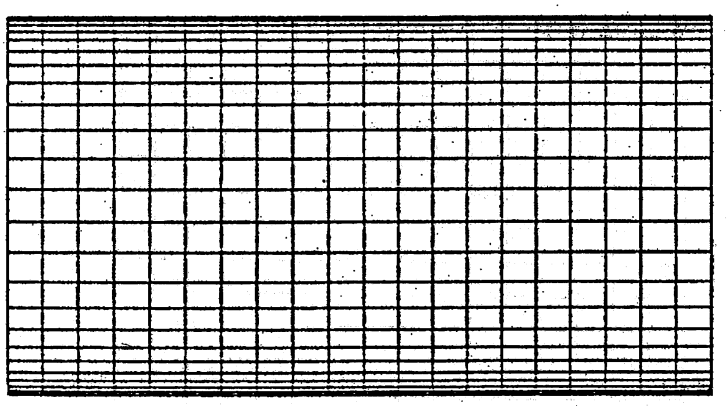

Figure II-5. Nonuniform hyperbolic mesh.